Design and Control of a Table-top Vibration Isolation System With Zero-power Gravity Compensation

Benjamin Friedl, Alexander Pechhacker, Ernst Csencsics, Georg Schitter
Automation and Control Institute (ACIN)
Technische Universität Wien
Vienna, Austria

***Abstract*—This paper presents the design, implementation and evaluation of a vibration isolation system with a magnetically levitated platform and tunable zero-power gravity compensation. The system, motivated by the stringent requirements of high-precision applications, employs Lorentz actuators for the platform's six degrees of freedom. Zero-power gravity compensation is achieved by electropermanent magnets, allowing adaptation to a varying payload while maintaining a constant operating point. Using decoupling transformations, the platform is stabilized by decentralized position control. For vibration isolation in the vertical direction, the position control bandwidth is reduced to 8 Hz by compensating the negative stiffness of the electropermanent magnets, resulting in an attenuation of floor vibrations with −40 dB/decade above this frequency. Acceleration feedback further reduces the transmissibility by 9.7 dB (67 %). The tunable gravity compensation supports a total load of 6.34 kg and reduces the power consumption of the Lorentz actuators by 98.9 %.**

***Index Terms*—active vibration isolation, gravity compensation, magnetic levitation, 6-DoF platform, mechatronics**

I. Introduction

Vibrations originate from various sources like human activity, traffic, heavy machinery or building motion, and are therefore present almost everywhere [1], [2]. Moreover, their intensity is increasing in areas such as automated production, driven by the demand for higher speeds and forces. This is especially challenging for processes that require positioning precision in the nanometer range, like the production of semiconductor components with lithographic wafer scanners. In this case, vibrations are not only transmitted from outside the plant (indirect disturbances), but also generated within (direct disturbances) due to the highly dynamic positioning processes with accelerations of up to 40 m/s^2 [3], [4]. Sophisticated vibration isolation strategies are also required in research, for example, to enable measurements at the atomic level with atomic force microscopes (AFM) [5], [6], the detection of gravitational waves with large-scale interferometers [7], and observations with large reflecting telescopes [8].

B. Friedl and E. Csencsics are with the Christian Doppler Laboratory for Precision Measurements in Motion, Automation and Control Institute, TU Wien.
Corresponding author: friedl@acin.tuwien.ac.at

Passive vibration isolation systems are one way to protect such sensitive equipment from mechanical disturbances. However, there are two significant design trade-offs: Firstly, employing a compliant suspension decreases the transmission of indirect disturbances but increases susceptibility to direct disturbances [9], [10]. Secondly, reducing damping results in a steeper roll-off of the transmissibility but amplifies the resonance peak. Another limitation results from the static deflection of the support structure due to gravity [11], [10]. Active control additionally requires sensors and actuators but can remedy these drawbacks [12], [13], [14]. Two common approaches are feedback and feedforward control using inertial sensors, which provide measurements with respect to an inertial (vibration-free) reference [15], [16]. Moreover, active vibration isolation is commonly combined with magnetic levitation, as the mechanical connection between the vibrating floor and the sensitive equipment is avoided [17], [18].

Levitation can be achieved with Lorentz actuators, which have a very low stiffness but require a constant power supply to lift the payload [19]. The resulting heat dissipation can affect high-precision applications that usually require a constant temperature [20]. A common alternative are permanent magnets, which do not require any energy [21], [17]. However, the weight of the payload is only compensated accurately at a certain distance. Thus, the arrangement of the permanent magnets must be adjusted when the payload or the operating point is changed [21], [22].

The contribution of this paper is the design and control of a compact vibration isolation system with a magnetically levitated platform that integrates electropermanent magnets (EPM) [23], [24] to enable zero-power gravity compensation for a variable payload while maintaining a constant operating point.

II. Design and Implementation

A. Concept and Requirements

The vibration isolation system is intended for table-top operation and consists of a static base and a levitating platform with six degrees of freedom (DoF), which carries the sensitive equipment. To stabilize all six DoFs of the platform, the

Pre-print version of the article: B. Friedl, A. Pechhacker, E. Csencsics, and G. Schitter, "Design and Control of a Table-top Vibration Isolation System With Zero-power Gravity Compensation," *2024 IEEE/ASME International Conference on Advanced Intelligent Mechatronics*, July 15th - 19th 2024, Boston, MA, USA, 2024.

same number of Lorentz actuators is used due to their low stiffness and linear characteristics. Typically, floor vibrations are small in amplitude, with major frequency components up to 150 Hz [6]. Therefore, the air gap of the actuators can be kept small, resulting in a higher motor constant and lower power consumption. With the targeted positioning range of $\pm 0.5\,\mathrm{mm}$ in the translational DoFs and $\pm 0.3°$ in the rotational DoFs of the platform, small manufacturing inaccuracies are tolerable.

Zero-power gravity compensation is achieved with EPMs, which can be tuned to a varying payload by applying sufficiently high current pulses [23], [25]. As the load may not be placed precisely at the center of the platform, three EPMs are required. Given the gravity compensation's limited capacity, the platform weight should be as low as possible to allow a higher payload. At the same time, however, the platform must be rigid enough to avoid structural modes within the control bandwidth. The minimum payload capacity is 3 kg, which is sufficient for measurement equipment like an AFM.

Active vibration isolation is implemented in the vertical direction since this is where ground vibrations primarily act, for a frequency range of 5 Hz to 100 Hz, which is usually the most critical in practical applications [2]. Higher-frequency disturbances are attenuated by the system dynamics, which are dominated by the inertia of the mass.

B. Mechanical Construction

The platform is depicted in Fig. 1 and consists of a circular disc of $\varnothing 250\,\mathrm{mm} \times 5\,\mathrm{mm}$, on which the movers of the six actuators are mounted. Most parts are manufactured from aluminum (EN AW-6061) for a low weight. An eigenfrequency analysis performed in SolidWorks shows that the first eigenmode occurs at 268 Hz, which is well above the desired control bandwidth of 100 Hz. A disc with the same dimensions and material is used for the base, which carries the displacement sensors and the actuator stators.

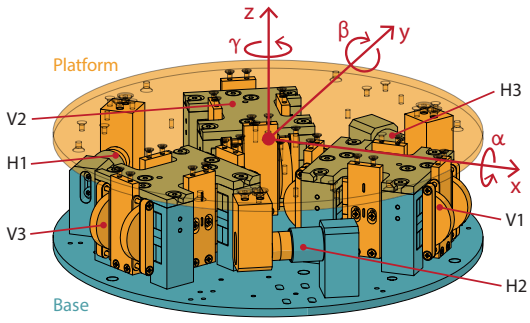

Fig. 1. 3D rendering of the vibration isolation system, showing the base (blue) and the levitating platform (orange). Actuators $V1$, $V2$, $V3$ are responsible for the out-of-plane DoFs (z, α, β), and $H1$, $H2$, $H3$ actuate the in-plane DoFs (x, y, γ).

C. Actuators

The three Lorentz actuators $V1$, $V2$ and $V3$ operate in the vertical direction and are arranged on a circle with an offset of 120° between each other, as shown in Fig. 2. They are responsible for the three out-of-plane DoFs (translation along the z-axis, and rotation around the x- and y-axis) and have an integrated EPM for gravity compensation [23]. The other three actuators $H1$, $H2$ and $H3$ are voice coils (AVM20-10, TDS Precision Products, Germany), which are oriented in the circumferential direction and actuate the in-plane DoFs (translation along the x- and y-axis, and rotation around the z-axis).

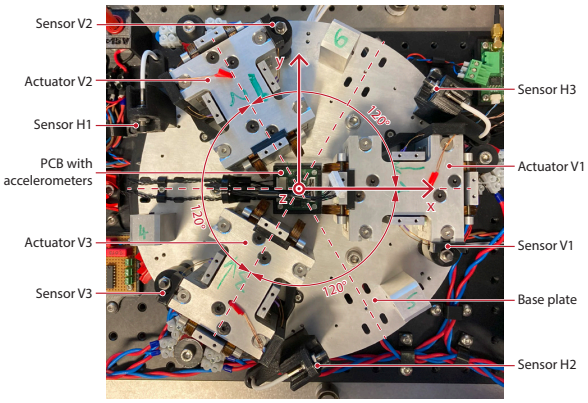

Fig. 2. Inside the vibration isolation system are three Lorentz actuators with an integrated EPM [23], six eddy-current displacement sensors, and accelerometers. The voice coil actuators are not mounted in the image.

D. Sensors

The displacement of the levitating platform is measured by six eddy-current sensors (eddyNCDT 3701-U1-A-C3, Micro-Epsilon Messtechnik, Germany), which require an aluminum target and have a measuring range of 1 mm. As shown in Fig. 2, they are placed close to the actuators to achieve collocation [16].

Two low-noise MEMS accelerometers (ADXL355, Analog Devices, USA) measure the vibrations both on the platform and the base. The circuit board mounted on the base can be seen in Fig. 2.

The gravity compensation can be tuned more easily by observing the flux density in the air gap of the EPMs [25]. For this purpose, they are equipped with a Hall sensor (HE144T, Asensor Technology, Sweden), which has a thickness of only 0.5 mm and can therefore be placed in the air gap.

E. Data Acquisition and Control

The control of the platform is implemented on a rapid-prototyping system (MicroLabBox DS1202, dSPACE, Germany). The position control and active vibration suppression run on a CPU with a clock frequency of 25 kHz. Due to the higher timing requirements, the control of the current pulse generator used to tune the EPMs is implemented on the FPGA, which runs at 100 MHz.

Pre-print version of the article: B. Friedl, A. Pechhacker, E. Csencsics, and G. Schitter, "Design and Control of a Table-top Vibration Isolation System With Zero-power Gravity Compensation," *2024 IEEE/ASME International Conference on Advanced Intelligent Mechatronics*, July 15th - 19th 2024, Boston, MA, USA, 2024.

III. Dynamic Model

For modelling the dynamics, the platform is treated as a rigid, free-floating body with six DoFs. Its position and orientation, measured in a coordinate system fixed to the base, is specified by the vector $\boldsymbol{x} = \begin{bmatrix} x & y & z & \alpha & \beta & \gamma \end{bmatrix}^{\mathrm{T}}$, where the angles α, β and γ denote the rotation around the axes x, y and z, respectively (see Figs. 1 and 2). The orthogonal forces and torques acting on the platform are expressed by the vector $\boldsymbol{u} = \begin{bmatrix} F_x & F_y & F_z & M_\alpha & M_\beta & M_\gamma \end{bmatrix}^{\mathrm{T}}$. Applying the Laplace transformation $\mathcal{L}\{\cdot\}$ to the equation of motion $M\ddot{\boldsymbol{x}} = \boldsymbol{u}$, where $M \in \mathbb{R}^{6\times6}$ is the invertible mass and inertia matrix, yields

$$\mathcal{L}\{\boldsymbol{x}\}(s) = \underbrace{\frac{1}{s^2} M^{-1}}_{G(s)} \mathcal{L}\{\boldsymbol{u}\}(s).$$

Assuming that the matrix M is diagonal and only contains the mass m and the principal moments of inertia J_x, J_y, J_z, gives the transfer function matrix

$$G(s) = \operatorname{diag}\left(\frac{1}{ms^2}, \frac{1}{ms^2}, \frac{1}{ms^2}, \frac{1}{J_x s^2}, \frac{1}{J_y s^2}, \frac{1}{J_z s^2}\right).$$

The superposition of the actuator forces $\boldsymbol{f} = \begin{bmatrix} F_{V1} & F_{V2} & F_{V3} & F_{H1} & F_{H2} & F_{H3} \end{bmatrix}^{\mathrm{T}}$ leads to the resulting forces and torques $\boldsymbol{u} = V\boldsymbol{f}$. The matrix $V \in \mathbb{R}^{6\times6}$ is determined by the arrangement of the actuators in relation to the platform's center of gravity. Since it is invertible, the actuator forces $\boldsymbol{f}$ are uniquely determined by $\boldsymbol{u}$, meaning that an arbitrary translation and rotation can be generated.

The forces of the Lorentz actuators are linearly related to the respective currents $\boldsymbol{i} = \begin{bmatrix} I_{V1} & I_{V2} & I_{V3} & I_{H1} & I_{H2} & I_{H3} \end{bmatrix}^{\mathrm{T}}$ by $\boldsymbol{f} = K_M\boldsymbol{i}$ with the diagonal motor constant matrix $K_M \in \mathbb{R}^{6\times6}$. Using the above equations, the currents required to apply a certain force or torque to the platform are $\boldsymbol{i} = K_M^{-1}\boldsymbol{f} = K_M^{-1}V^{-1}\boldsymbol{u}$.

Assuming that the displacement of the platform from its center position $\boldsymbol{x} = \boldsymbol{0}$ is small, the sensor signals $\boldsymbol{y} = \begin{bmatrix} y_{V1} & y_{V2} & y_{V3} & y_{H1} & y_{H2} & y_{H3} \end{bmatrix}^{\mathrm{T}}$ can be approximated by the linear transformation $\boldsymbol{y} = W\boldsymbol{x}$. The matrix $W \in \mathbb{R}^{6\times6}$ is determined by the arrangement of the sensors with respect to the platform's center of gravity. By inverting W, $\boldsymbol{x}$ can be uniquely calculated from $\boldsymbol{y}$.

IV. Control Design

As Fig. 3 shows, there are three controllers active in the z-axis of the vibration isolation system, which is represented by the transfer function $G_z(s)$. Firstly, a position controller $R_{p,z}(s)$ is required to keep the platform at its operating point (see Section IV-A). Secondly, an active attenuation of vibrations is achieved by feeding back the acceleration of the platform through the controller $R_a(s)$ (see Section IV-C).

While the position controller creates a stiff connection between the base and the platform within the control bandwidth, the acceleration feedback controller tries to suppress any motion of the platform with respect to an inertial reference. Due to these opposing goals, they should only be active in separate frequency ranges. Consequently, the cutoff frequency of the position control sets a lower limit for the bandwidth of the acceleration feedback. This also means that the bandwidth of the position control must be chosen to be small to enable vibration suppression at low frequencies. However, this is limited by the negative stiffness of the EPMs. For this reason, the third controller $R_s(s)$ is added to compensate the negative stiffness at the operating point (see Section IV-B).

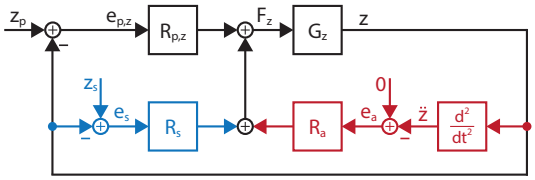

Fig. 3. Control loop of the platform's z-coordinate (represented by G_z) comprising the position controller $R_{p,z}$ (black), the virtual positive stiffness R_s (blue) and the acceleration feedback controller R_a (red).

A. Position Control

To stabilize the levitating platform at the operating point, position control with a cascaded structure is used [19]. The outer loop contains the position controller and is implemented on the rapid-prototyping system. The inner loop has a significantly higher bandwidth (10 kHz) and maintains the currents in the Lorentz actuators. The analog current controllers are implemented on external circuit boards.

Since the platform can be positioned in six DoFs by the six actuators, it is a multi-input multi-output (MIMO) system. In general, the position controller design must take into account the cross-coupling of the sensors and actuators. However, by transforming the actuator forces and sensor signals into an orthogonal coordinate system (see Section III), six independent single-input single-output (SISO) controllers can be used [26]. Thus, the position controller is given by the following diagonal matrix

$$R_p(s) = \operatorname{diag}\Big(R_{p,x}(s), R_{p,y}(s), \ldots, R_{p,\gamma}(s)\Big).$$

For the six SISO position controllers proportional-integral-derivative (PID) control is used [16]. The tuning according to [27] requires knowledge of the platform's frequency behavior, which can only be identified in closed-loop operation due to the levitation. Since this requires a stable position controller, the initial tuning is based on the mathematical model from Section III [19].

The identification is done according to [28] and yields in total 36 transfer functions. Six of them describe the dynamics of the main axes, and are used for the controller tuning. The other 30 represent the crosstalk between the DoFs. Evaluating the relative gain array (RGA) [26], reveals a sufficiently low cross-coupling that justifies the decentralized control approach.

B. Virtual Stiffness

The supply wires of the actuator coils and accelerometers result in a small positive stiffness in the vertical direction

Pre-print version of the article: B. Friedl, A. Pechhacker, E. Csencsics, and G. Schitter, "Design and Control of a Table-top Vibration Isolation System With Zero-power Gravity Compensation," *2024 IEEE/ASME International Conference on Advanced Intelligent Mechatronics*, July 15th - 19th 2024, Boston, MA, USA, 2024.

(dashed blue Bode plot in Fig. 4). However, the overall stiffness becomes negative when the flux density in the EPMs is increased (solid blue Bode plot in Fig. 4). In this case, there is still a spring line present, but the phase starts at −180°. Consequently, the crossover of the PID position controller must be placed on the mass line in order to be able to generate the phase margin required for stability [16]. This sets a lower limit for the bandwidth of the position controller. Therefore, an additional proportional controller $R_s = k_s \geq 0$ is added in the z-axis to compensate the negative stiffness at the operating point z_s (see Fig. 3).

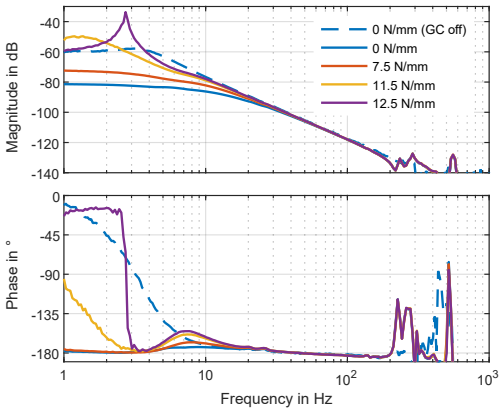

Fig. 4. Bode plots of the plant seen by the position controller $R_{p,z}(s)$ for different values of the gain k_s. The gravity compensation (GC) is tuned to carry the weight of the platform (1.88 kg). For the dashed blue Bode plot it is disabled.

The solid Bode plots with $k_s > 0$ in Fig. 4 show that the independent position feedback increases the effective stiffness of the plant seen by the position controller $R_{p,z}(s)$. With $k_s = 11.5\,\mathrm{N/mm}$ a good compensation is achieved, and the mass line starts already at about 2 Hz. If k_s is increased further, the negative stiffness is overcompensated, resulting in a resonance peak and phase shift (solid violet Bode plot in Fig. 4).

C. Acceleration Feedback

The acceleration feedback controller $R_a(s) = g_a\, H_a(s)$ generates a virtual mass equal to the gain g_a within a frequency range that is defined by the filter $H_a(s)$. It comprises low- and high-pass filters as well as filters for structural modes, which ensure the separation from the position controller and the stability of the feedback loop. The design is based on the frequency response of the platform in z-direction $s^2 G_z(s)$, shown in Fig. 5. Since it is the second derivative of a mass-spring-damper system, the magnitude first increases with frequency (corresponding to the spring line) and then continues horizontally (corresponding to the mass line), followed by structural modes at around 300 Hz. The phase decreases from initially 180° to 0° and is further reduced at higher frequencies due to the phase lag of the accelerometer. Fig. 5 also shows the Bode plots of the designed controller $R_a(s)$ for a gain $g_a = 4.5\,\mathrm{kg}$, and the open control loop $s^2 G_z(s) R_a(s)$. Noteworthy are the two crossings of the 0 dB-line, where a sufficient phase margin has to be ensured for stability.

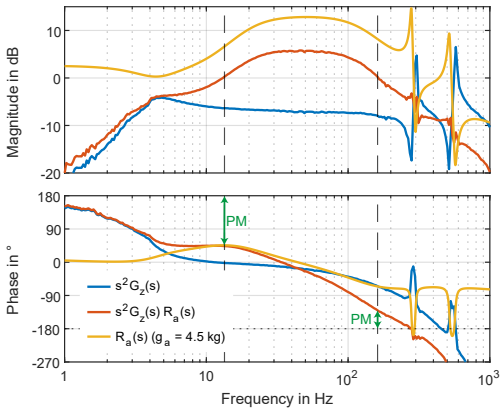

Fig. 5. Bode plots of the acceleration feedback controller $R_a(s)$ for the gain $g_a = 4.5\,\mathrm{kg}$, the plant $s^2 G_z(s)$ seen by the controller (measured with the accelerometer), and the open control loop $s^2 G_z(s) R_a(s)$. The phase margins (PM) at the two crossovers are indicated by the green double arrows.

The effect of position control and acceleration feedback on the transmissibility of disturbances from the base (z_0) to the platform (z) can be investigated using the following expression

$$\mathcal{L}\{z\} = \underbrace{\mathcal{T}_z \mathcal{L}\{z_0\}}_{\substack{\text{transmitted}\\ \text{vibrations}}} + \underbrace{G_z R_{p,z}(\mathcal{L}\{z_0\} - \mathcal{L}\{z\})}_{\text{response to position feedback}} + \ldots$$
$$\underbrace{G_z R_a (0 - s^2 \mathcal{L}\{z\})}_{\text{response to acceleration feedback}}.$$

The displacement of the platform in z-direction results from the vibrations transmitted due to the transmissibility of the passive system $\mathcal{T}_z(s)$, and the response to the position and acceleration feedback. Assuming $G_z(s) = \frac{1}{ms^2+cs+k}$ and $\mathcal{T}_z(s) = \frac{cs+k}{ms^2+cs+k}$ with k and c as spring and damping coefficients of the passive system, yields the transmissibility of the active system

$$\frac{\mathcal{L}\{z\}}{\mathcal{L}\{z_0\}} = \frac{cs + k + R_{p,z}}{\underbrace{(m + R_a)}_{\text{effective mass}} s^2 + cs + \underbrace{k + R_{p,z}}_{\text{effective stiffness}}}.$$

This shows that the position controller $R_{p,z}(s)$ increases the effective stiffness, and thereby causes the transmission of floor vibrations within the position control bandwidth. The acceleration feedback controller $R_a(s)$, on the other hand, adds a virtual mass, which reduces the transmissibility within the bandwidth determined by $H_a(s)$.

V. Evaluation of the System Performance

The performance of the system is characterized by its ability to lift an arbitrary payload (up to a certain maximum weight) without significant power consumption and the attenuation of floor vibrations.

Pre-print version of the article: B. Friedl, A. Pechhacker, E. Csencsics, and G. Schitter, "Design and Control of a Table-top Vibration Isolation System With Zero-power Gravity Compensation," *2024 IEEE/ASME International Conference on Advanced Intelligent Mechatronics*, July 15th - 19th 2024, Boston, MA, USA, 2024.

A. Gravity Compensation

To determine the power savings achieved with gravity compensation, it is first disabled and the static currents of the Lorentz actuators required to lift the platform and the payload are measured. Then the EPMs are tuned so that the weight of the load is compensated, and the currents of the Lorentz actuators are measured again. This procedure is performed with the platform only (1.88 kg), and with an additional payload of 4.46 kg, resulting in a total load of 6.34 kg. The power is calculated from the measured currents and the resistance of the actuator coils.

The results in Table I show that the current and power consumption are significantly lower in the compensated case. However, they are not exactly zero because the EPMs are manually tuned, and mutual forces occur between the six actuators due to the limited accuracy of the decoupling transformation. Nevertheless, the power consumption is reduced by 96.8 % and 98.9 %, respectively.

TABLE I
AVERAGE ACTUATOR CURRENT, TOTAL POWER CONSUMPTION, AND POWER SAVINGS WITH GRAVITY COMPENSATION FOR TWO LOAD CASES.

Total load m kg	Gravity compensation	Average current mA	Power consumption W	Power savings %
1.88	off	221	3.24	
	on	38	0.10	96.8
6.34	off	800	42.36	
	on	82	0.48	98.9

B. Vibration Isolation

The performance in terms of vibration isolation is evaluated by determining the transmissibility of disturbances from the base to the levitating platform. For this purpose, the base frame is excited while the inertial sensors measure the acceleration of the base and the platform. By taking the ratio of the Fourier-transformed time signals, the transmissibility is obtained as a function of frequency.

The experiments are performed for the same two load cases as in Section V-A, and varying values of the acceleration feedback gain g_a. The position controller for the z-axis is designed with a crossover frequency of 6 Hz. The bandwidth cannot be reduced further because the stiffness compensation is not robust enough. The reason for this is that the negative stiffness of the EPMs depends non-linearly on the position and is only compensated accurately at the operating point.

As can be seen from the results of the first experiment in Fig. 6a, up to 8 Hz the transmissibility is close to 0 dB because the position controller transmits floor vibrations to the platform within its bandwidth. Above the cutoff frequency, the transmissibility decreases by approximately 40 dB/decade due to the inertia of the platform mass. For the second load case, again an additional payload of 4.46 kg is added, and the gravity compensation is tuned accordingly. Due to the increased mass of the system, it is not excited sufficiently below 5 Hz, which is why the transmissibility is below 0 dB in this frequency range, as shown in Fig. 6b.

From the results, it can be seen that in both load cases, the mass line is shifted down with the acceleration feedback. Ideally, this shift is given by the effective mass ratio $v = m/(m + g_a)$, since the gain g_a acts as an additional virtual mass (see Section IV-C). The values obtained from fitting a mass line to the measurements are provided in Table II, and show good agreement with the theoretical values.

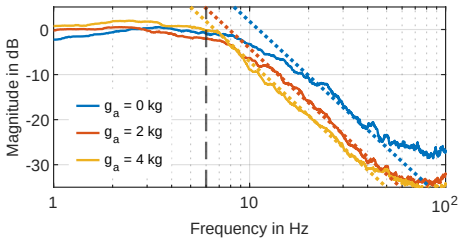

(a) Only platform (1.88 kg), without gravity compensation.

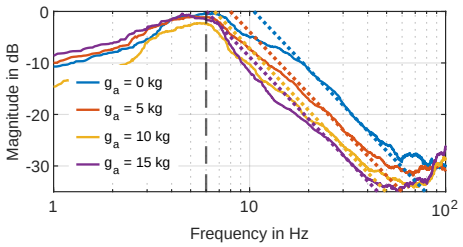

(b) Platform and payload (6.34 kg), with gravity compensation.

Fig. 6. Transmissibility of disturbances from the base to the platform for two load cases and different values of the acceleration feedback gain g_a. The position controller for the z-axis is tuned with a crossover frequency of 6 Hz (dashed black line). The dotted lines indicate the fitted mass lines.

TABLE II
MASS RATIO WITH ACTIVE VIBRATION ISOLATION FOR TWO LOAD CASES AND DIFFERENT VALUES OF THE ACCELERATION FEEDBACK GAIN g_a.

Total load m kg	Feedback gain g_a kg	Theoretical mass ratio v	dB	Fitted mass ratio	dB
1.88	2	0.48	-6.3	0.50	-6.0
	4	0.32	-9.9	0.36	-8.9
6.34	5	0.56	-5.1	0.57	-4.8
	10	0.39	-8.2	0.40	-8.1
	15	0.30	-10.5	0.33	-9.7

In summary, it is successfully demonstrated that by tuning the EPMs of the designed vibration isolation system, the static power consumption of the Lorentz actuators is reduced by almost 99 % for a total payload of 6.34 kg. Moreover, the transmissibility of floor vibrations decreases above 8 Hz with 40 dB/decade, and is further reduced by −9.7 dB (≈ 67 %) using acceleration feedback.

Pre-print version of the article: B. Friedl, A. Pechhacker, E. Csencsics, and G. Schitter, "Design and Control of a Table-top Vibration Isolation System With Zero-power Gravity Compensation," *2024 IEEE/ASME International Conference on Advanced Intelligent Mechatronics*, July 15th - 19th 2024, Boston, MA, USA, 2024.

VI. Conclusion

The Lorentz actuators with integrated EPMs enable the implementation of a compact vibration isolation system. Using suitable decoupling transformations, the levitating 6-DoF platform can be stabilized at the operating point by decentralized PID position control. Tuning the gravity compensation to the weight of the payload, results in a reduction of the static power consumption by almost 99 %. The cutoff frequency of the transmissibility is mainly determined by the position control bandwidth, for which a lower limit is set by the negative stiffness of the EPMs. Adding a positive stiffness to the system by an additional controller, allows a reduction of the bandwidth to 8 Hz. Above this frequency, floor vibrations are attenuated with −40 dB/decade. It is also demonstrated how the acceleration feedback increases the effective mass, thereby shifting the mass line of the transmissibility down. When designing the controller, it must be ensured that the bandwidth is separated from that of the position controller, and that there is a sufficient phase margin at the two crossovers. With the implemented controller, the transmissibility is further reduced by −9.7 dB ($\approx 67\,\%$).

Future work includes the reduction of the position control bandwidth by using a more robust stiffness compensation, the automatic tuning of the EPMs according to the weight of the payload, and the implementation of more sophisticated active vibration isolation approaches, like disturbance feedforward.

Acknowledgement

The financial support by the Austria Wirtschaftsservice (AWS) as well as by the Austrian Federal Ministry of Labour and Economy, the National Foundation for Research, Technology and Development and the Christian Doppler Research Association is gratefully acknowledged.

References

[1] H. Bachmann and W. Ammann, *Vibrations in Structures: Induced by Man and Machines*, ser. Structural Engineering Documents. Zürich, Switzerland: International Association for Bridge and Structural Engineering, 1987, vol. 3e.

[2] E. I. Rivin, *Passive Vibration Isolation*. New York, NY, USA: ASME Press, 2003.

[3] M. F. Heertjes, H. Butler, N. J. Dirkx, S. H. van der Meulen, R. Ahlawat, K. O'Brien, J. Simonelli, K.-T. Teng, and Y. Zhao, "Control of Wafer Scanners: Methods and Developments," in *Proceedings of the 2020 American Control Conference (ACC)*, 2020, pp. 3686–3703.

[4] H. Butler, "Position Control in Lithographic Equipment: An Enabler for Current-Day Chip Manufacturing," *IEEE Control Systems Magazine*, vol. 31, no. 5, pp. 28–47, 2011.

[5] S. Ito, J. Steininger, and G. Schitter, "Low-stiffness dual stage actuator for long rage positioning with nanometer resolution," *Mechatronics*, vol. 29, pp. 46–56, 2015.

[6] S. Ito, S. Unger, and G. Schitter, "Vibration isolator carrying atomic force microscope's head," *Mechatronics*, vol. 44, pp. 32–41, 2017.

[7] R. DeRosa, J. C. Driggers, D. Atkinson, H. Miao, V. Frolov, M. Landry, J. A. Giaime, and R. X. Adhikari, "Global feed-forward vibration isolation in a km scale interferometer," *Classical and Quantum Gravity*, vol. 29, no. 21, pp. 215 008–215 020, 2012.

[8] B. Sedghi, P. Zuluaga-Ramírez, U. Lampater, D. Pilbauer, S. Leveratto, G. Jakob, M. Müller, J. Abad-Pastor, J. C. González-Herrera, and S. Patti, "ESO ELT - vibration sources characterization: a step forward towards requirement and performance verification," in *Modeling, Systems Engineering, and Project Management for Astronomy IX*, 2020, pp. 27–39.

[9] M. A. Beijen, "Disturbance feedforward control for vibration isolation systems: analysis, design, and implementation," Ph.D. dissertation, Technische Universiteit Eindhoven, Eindhoven, 2018.

[10] P. K. Subrahmanyan, "A Modal Approach to Precision Motion Control," Ph.D. dissertation, Massachusetts Institute of Technology, Cambridge, MA, USA, 1999.

[11] C. M. Harris and A. G. Piersol, Eds., *Harris' Shock and Vibration Handbook*, 5th ed. New York, NY, USA: McGraw-Hill, 2002.

[12] D. Karnopp, M. J. Crosby, and R. A. Harwood, "Vibration Control Using Semi-Active Force Generators," *Journal of Engineering for Industry*, vol. 96, no. 2, pp. 619–626, 1974.

[13] A. Preumont, M. Horodinca, I. Romanescu, B. de Marneffe, M. Avraam, A. Deraemaeker, F. Bossens, and A. Abu Hanieh, "A six-axis single-stage active vibration isolator based on Stewart platform," *Journal of Sound and Vibration*, vol. 300, no. 3-5, pp. 644–661, 2007.

[14] C. R. Fuller, *Active Control of Vibration*. Oxford, U.K.: Elsevier Science & Technology, 1996.

[15] C. Collette, S. Janssens, and K. Artoos, "Review of Active Vibration Isolation Strategies," *Recent Patents on Mechanical Engineering*, vol. 4, no. 3, pp. 212–219, 2011.

[16] R. M. Schmidt, G. Schitter, A. Rankers, and J. van Eijk, *The Design of High Performance Mechatronics: High-Tech Functionality by Multidisciplinary System Integration*, 2nd ed. Amsterdam, Netherlands: IOS Press under the imprint Delft University Press, 2014.

[17] T. Zhu, B. Cazzolato, W. S. Robertson, and A. Zander, "Vibration isolation using six degree-of-freedom quasi-zero stiffness magnetic levitation," *Journal of Sound and Vibration*, vol. 358, pp. 48–73, 2015.

[18] M. E. Hoque and T. Mizuno, "Magnetic levitation technique for active vibration control," in *Magnetic Bearings*, B. Polajzer, Ed. Rijeka, Croatia: Sciyo, 2010.

[19] D. Wertjanz, E. Csencsics, J. Schlarp, and G. Schitter, "Design and control of a MAGLEV platform for positioning in arbitrary orientations," in *2020 IEEE/ASME International Conference on Advanced Intelligent Mechatronics (AIM)*. Piscataway, NJ: IEEE, 2020, pp. 1935–1942.

[20] S. Hol, E. Lomonova, and A. Vandenput, "Design of a magnetic gravity compensation system," *Precision Engineering*, vol. 30, no. 3, pp. 265–273, 2006.

[21] J. Janssen, J. Paulides, E. A. Lomonova, B. Delinchant, and J.-P. Yonnet, "Design study on a magnetic gravity compensator with unequal magnet arrays," *Mechatronics*, vol. 23, no. 2, pp. 197–203, 2013.

[22] M. Raab, M. Hutter, A. Kazi, W. Schinkoethe, and B. Gundelsweiler, "Magnetically Levitated Linear Drive Using an Active Gravity Compensation Based on Hybrid Shape Memory Actuators," *IEEE/ASME Transactions on Mechatronics*, vol. 26, no. 3, pp. 1380–1391, 2021.

[23] A. Pechhacker, D. Wertjanz, E. Csencsics, and G. Schitter, "Integrated electromagnetic actuator with adaptable zero power gravity compensation," *IEEE Transactions on Industrial Electronics*, pp. 1–9, 2023.

[24] A. N. Knaian, "Electropermanent Magnetic Connectors and Actuators: Devices and Their Application in Programmable Matter," Ph.D. dissertation, Massachusetts Institute of Technology, Cambridge, MA, USA, 2010.

[25] A. Pechhacker, D. Wertjanz, E. Csencsics, and G. Schitter, "Model-based flux control of an electropermanent magnet for adaptive zero power gravity compensation," *IFAC-PapersOnLine*, vol. 56, no. 2, pp. 5352–5357, 2023.

[26] S. Skogestad and I. Postlethwaite, *Multivariable Feedback Control: Analysis and Design*, 2nd ed. Chichester: John Wiley & Sons, 2005.

[27] E. Csencsics and G. Schitter, "Parametric PID controller tuning for a fast steering mirror," in *Proceedings of the 2017 IEEE Conference on Control Technology and Applications (CCTA)*, 2017, pp. 1673–1678.

[28] E. Wernholt and S. Gunnarsson, "On the use of a multivariable frequency response estimation method for closed loop identification," in *Proceedings of the 43rd IEEE Conference on Decision and Control*, 2004, pp. 827–832 Vol.1.

Pre-print version of the article: B. Friedl, A. Pechhacker, E. Csencsics, and G. Schitter, "Design and Control of a Table-top Vibration Isolation System With Zero-power Gravity Compensation," *2024 IEEE/ASME International Conference on Advanced Intelligent Mechatronics*, July 15th - 19th 2024, Boston, MA, USA, 2024.